

UDC 666.646

MECHANICAL AND MICROSTRUCTURAL PROPERTIES OF OPAQUE CERAMIC TILES GLAZED WITH SOME INDUSTRIAL WASTES

Lina İ. İsrail¹Abstract published in *Steklo i Keramika*, No. 8, pp. 66–67, August, 2022.*Original article submitted December 29, 2021.*

The primary goal of this research is to determine the mechanical properties of opaque glazed ceramic tiles containing fly ash, tincal waste, and recycled red clay, including to assess if the results meet international requirements. Opaque glaze and tincal waste were the main components of all glaze compositions of four groups, which were named OG (original), FA, RC, and FC (mixture) according to the additive. The ceramic tiles were prepared by dipping the biscuits in the glaze composition and firing them at 1150°C. The water absorption of the FA, RC, and FC tiles was less than that of the OG tiles (< 0.52%) and the scratch hardness values were between 6 and 7. All the experimental groups were also resistant to thermal shock, chemicals, and staining showing high opacity ($L^* > 92$) and having a light yellow–red color. The micro- and crystallographic structure of some selected tiles were determined by scanning electron microscopy and x-ray diffraction techniques. Zircon, diopside and augite phases were recognized.

Keywords: opaque glaze, fly ash, tincal waste, red clay.

INTRODUCTION

The rapid growth of the population has caused mankind to look for new industrial branches with technological developments. The rise in production increases the deposition of wastes and its associated costs while depleting the number of natural resources by damaging the natural environmental [1]. According to the recent data regarding urbanization and growth rates, 1.3 billion tons of waste is created every year, with 1 million per day only in Asia alone [2]. In addition to being an alternative for natural raw materials, reusing and recycling of the waste [3] would increase the variety of the products, conserve energy by lowering the cost of production, minimize the pollution worldwide [4–6].

Glazes are the permanent covering vitrified on the surface of a ceramic body by firing [7] which are classified as raw and frit according to the origin of oxides they contain. Raw glaze oxides are in the form of minerals or compounds, whereas the frit glaze oxides are in the frit form- insoluble glass [8]. Opaque glaze is a type of glaze that is produced when a material is mixed to a homogeneous glaze forming another phase other than the vitreous state in the glass [9] and is used to achieve lustrous surfaces. The ceramic indus-

try, especially glaze [10], is a viable alternative for disposing of wastes [11].

Fly ash (FA), an alumina silicate powdered residue of coal combustion at high temperatures [12], is a threat to ecology [13]. For instance, in Turkey 55 million tons of coal is used up in coal thermal power plants every year, generating approximately 13 million tons of fly ash; however, only 1% is exploited, creating a significant problem both economically and environmentally [14]. The reuse of fly ash in different areas, such as cement [15], bricks [16], ceramics [17], glass, and glass-ceramics [18] is increasing daily.

Red clay (RC) is a combination of minerals consisting of silica, alumina, and ferric oxide as the main components. Its plasticity and porosity properties are quite good in that it can replace clay minerals, such as in pottery [19] and tile manufacturing [20, 21] improving mechanical properties. In the ceramic industry, masse and glazes are prepared by clay minerals, where expensive fluxing oxides might be needed [10]. Thus, red clay may be used instead of clay minerals, where ferric oxide in red clay will be a good fluxing agent if used in certain amounts.

Boron reserves are abundant in Turkey, a country tincal is one of the ores mined. Tincal is purified into boric acid and/or borax derivatives with one million tons of production and more than one hundred thousand tons of waste per year.

¹ Ege Vocational School, Ege University, 35040, İzmir, Turkey.

TABLE 1. Chemical Analysis of OG

Oxide	SiO ₂	Al ₂ O ₃	CaO	MgO	Na ₂ O	K ₂ O	ZrO ₂	ZnO
Amount, %	54.46	10.65	11.89	3.24	4.89	2.84	5.08	6.95

TABLE 2. The Molecular Unit Formula of OG

0.16 Na ₂ O								
0.06 K ₂ O			1.86 SiO ₂					
0.43 CaO	0.21 Al ₂ O ₃							
0.17 MgO			0.08 ZrO ₂					
0.18 ZnO								

Borax compounds in tincal waste (TW) readily dissolves in rain waters and penetrate into the ground and into groundwater if they are left exposed, thus, creating severe problems for the environment and human health [22]. These compounds also consist of boron oxide, a good fluxing oxide that has a tendency to lower the softening temperature of the glazes. Therefore, the utilization of TW in glazes will be a solution for lowering the costs of production and detrimental effects.

The mechanical properties of the glazed ceramic tiles containing FA, RC, and TW and their consistency with international standards were investigated. Water absorption (WA), scratch hardness (SH), thermal shock resistance (TSR), resistance to chemicals, resistance to staining, and color difference tests were performed. The surface microstructure and surface crystalline phases of the glazed tiles were analyzed by scanning electron microscopy (SEM) and x-ray diffraction (XRD).

EXPERIMENTAL

Characterization of the OG

Ege Seramik Inc. (Izmir, Turkey) supplied the standard OG. The chemical analysis of OG is given in Table 1. The x-ray fluorescence (XRF) technique was performed using the

Metek Spectra IQ II XRF spectrometer for the chemical analysis. The chemistry of the glaze recipe can also be evaluated using the molecular unit formula (Table 2), which shows both the mole ratio between fluxing oxides and the ratio of the total moles of fluxes (which is 1) to the moles of silica and alumina. This formula is calculated according to the chemical analysis of OG. The particle size distribution analysis of wet sieving is shown in Table 3.

The thermal behavior of the dried OG (Fig. 1) between 400 and 1300°C was analyzed by using a hot stage microscope (Misura 3.32) at Ege Seramik Inc. (Izmir, Turkey). The sintering, softening, and melting temperatures were measured as 906, 1060, and 1214°C respectively.

Characterization of wastes

Absolute densities of dried FA (Tunçbilek Thermal Plant-Kütahya, Turkey), TW (Etibank Boron Plant-Eskişehir, Turkey) and RC (Ikizler Seramik-Menemen, Izmir) were determined using the pycnometer method. All samples were ground in a ball mill and sieved for particle size distribution analysis (Table 4). The chemical compositions of FA and RC were established with the same XRF instrument mentioned above. A Rikagu NEXCG (Pd anode) XRF spectrometer (Ege University-Izmir, Turkey) was utilized for TW (Table 5).

To understand the plasticity character of RC, the Pfefferkorn method [23, 24] was used and for flowability character, the Hausner ratio [25] was determined.

Preparation and characterization of the tiles

OG and the waste materials were used in four different batches (Table 6); OG, FA, RC, FC. OG is the standard opaque glaze. FA and RC glazes contain different percentages of the waste. FC glazes contain both FA and RC. The

TABLE 3. The Particle Size Distribution of OG

Wet sieve fraction, μm	< 32	32 – 45	45 – 63	63 – 100	100 – 150	150 – 300	300 – 600	Total
Amount, %	72.49	21.87	0.85	1.28	1.74	0.93	0.84	100

TABLE 4. The Particle Size Distribution of Wastes

Wet sieve fraction, μm	< 32	32 – 45	45 – 63	63 – 100	100 – 150	150 – 300	300 – 600	Total
FA	57.19	12.06	12.76	16.54	0	0	0.45	100
TW	56.10	19.50	13.97	8.61	1.82	0	0	100
RC	49.28	24.03	25.21	0.34	0	0	0.14	100

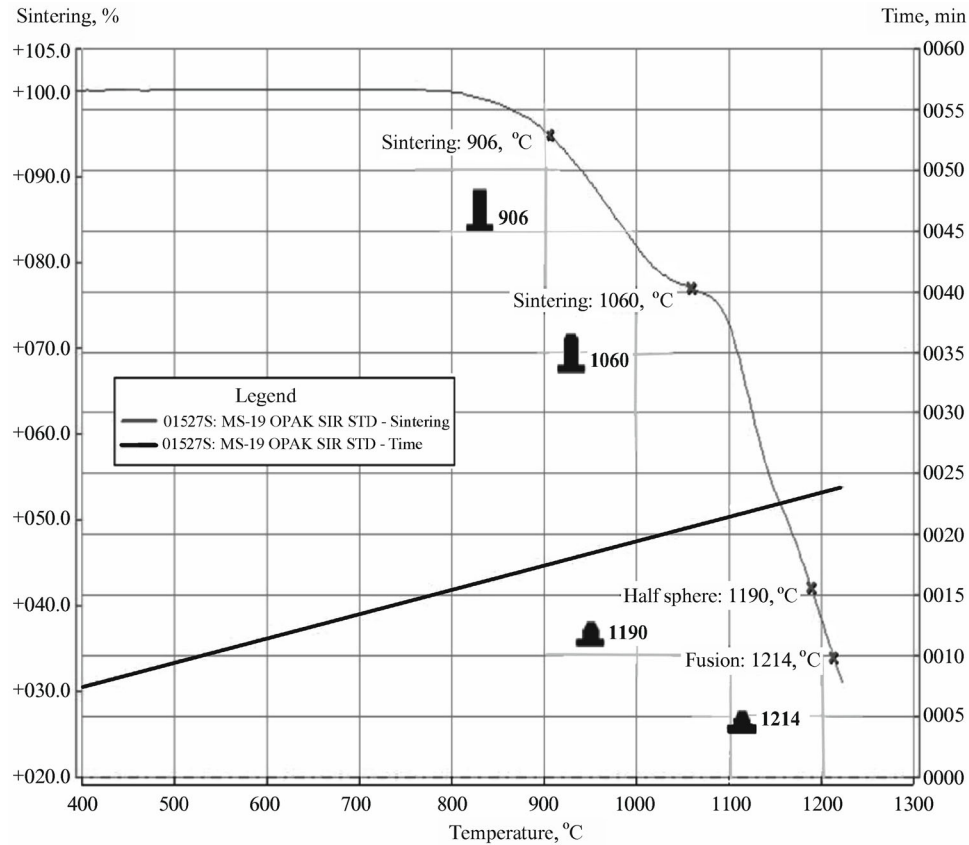


Fig. 1. Thermal behavior of OG.

names of the batches are expressed with the percentage of the raw material. Five percent of TW was added to each group to decrease the sintering temperature.

In dipping glazes, the sucking of water by the biscuit tile causes the thickening of the glaze. Therefore, the density and the viscosity of the glaze mixtures should be arranged before

dipping. The specific gravities were measured by using pycnometers and flow times were measured by a Ford Cup (PCE 127/4) with an orifice diameter of 4 mm to control the kinematic viscosity of the batches. The pH values of all batches were measured by an ATC-pH meter. Each batch was stirred for two hours under a mechanical stirrer

TABLE 5. Chemical Compositions of Wastes

Amount, %	SiO ₂	Al ₂ O ₃	CaO	MgO	Na ₂ O	K ₂ O	Fe ₂ O ₃	B ₂ O ₃	LOI*
FA	56.16	19.00	3.44	4.33	0.07	1.85	12.36	0	1.88
TW	16.70	0	17.70	10.70	16.85	0	0	38.05	0
RC	54.69	18.54	3.21	1.94	0.81	3.31	8.08	0	9.42

* LOI: Loss of ignition.

TABLE 6. Body Compositions of the Batches (%)

Batch name	OG	FA0.5	FA1	FA2	FA3	FA4	RC0.5	RC1	RC2	RC3	RC4	F4C0.5	F0.5C4	F2C2
OG	95	94.5	94	93	92	91	94.5	94	93	92	91	90.5	90.5	91
FA	0	0.5	1	2	3	4	0	0	0	0	0	4	0.5	2
TW	5	5	5	5	5	5	5	5	5	5	5	5	5	5
RC	0	0	0	0	0	0	0.5	1	2	3	4	0.5	4	2

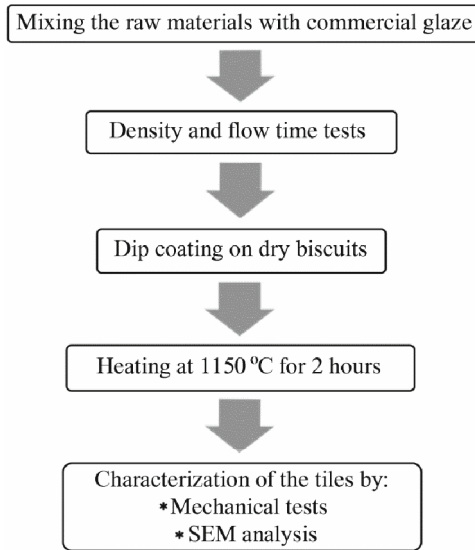


Fig. 2. The flowchart of the experimental procedure.

(IKA RW 28). The mixtures were applied to dried biscuit tiles with dimensions of $5 \times 5 \times 1 \text{ cm}^3$. The excessive glaze under the tiles and on both sides was cleaned carefully and left for 24 h in a drying oven (Heraeus). After that, the tiles were heated at 1150°C for 2 h (Protherm PAF120/12). Both the heating and cooling rates were 25 K/min . Then, the tiles were prepared for mechanical tests and SEM analysis now. The procedure is summarized by a flowchart in Fig. 2.

WA test [26]: The dried tiles with constant masses (m_1) were boiled for two hours in a container. After cooling to room temperature, they were dried with a clean cloth and weighed (m_2). WA was calculated according to Eq. (1) below:

$$\% \text{ WA} = \frac{m_1 - m_2}{m_1} \times 100\%. \quad (1)$$

SH test [27]: The SH test was performed by Ege Seramik Inc. (Izmir, Turkey). The surfaces of the glazed tiles of each batch were scratched by the sharp edge of the reference minerals with different Mohs' hardnesses. The procedure was repeated four times with new edges. The SH of the sample was compared with reference minerals.

TSR (Harcourt) test [28]: This method is based on keeping the glazed bodies in a hot oven for twenty minutes, and then immersing them in cold water at $15 \pm 5^\circ\text{C}$ for ten minutes. The formation of fine cracks on the surfaces of tiles was tested by 1% (w/w) methylene blue solution after they were dried with a clean cloth. The temperature of the oven was raised 20°C each time if no cracks were detected. The existence of the cracks was controlled between 100 and 200°C .

Resistance to chemicals [29]: Five samples of each batch were kept separately in dilute (3% (v/v) HCl and 1 g/L KOH) and concentrated (18% (v/v) HCl and 30 g/L KOH)

chemicals for four days. The outlook comparison was made between the tested and untested bodies.

Resistance to staining [30]: The staining sources (green material, olive oil, and iodine solution) were wiped on the tiles and left for 24 h; then they were classified according to the removal of stains by hot water or a chemical.

Color [31] and glossiness tests: L^* , a^* , and b^* trichromatic color values according to CIELab Color System were measured using Erichsen Spectromaster 565 D, and the gloss values were specified with Minolta Gloss 268 instrument in Ege Seramik Factory (Izmir, Turkey).

L^* is the whiteness (opacity) ranging between 0 and 100. a^* is the color variation between green (negative values) and red (positive values) where b^* is between blue (negative values) and yellow (positive values). The average of three measurements was calculated as the L^* , a^* , and b^* coordinates. The color difference (ΔE^*) between standard OG and each sample of the batches was calculated with Eq. (2). The ΔE^* value should be less than 1 [32].

$$\Delta E^* = \sqrt{(L_1^* - L_2^*)^2 + (a_1^* - a_2^*)^2 + (b_1^* - b_2^*)^2}. \quad (2)$$

The numbers 1 and 2 represent sample and standard respectively. The angle of the incident beam from the gloss meter on the glazed surface was 60° .

SEM analysis: The microstructures of the glazed tiles were clarified by a Thermo Scientific Apreo low vacuum SEM instrument (Ege University) operating at 10–500 Pa vacuum pressure and 0.8 nm resolution and with an ET (Everhart–Thornley) detector.

XRD analysis: The crystal phases were identified using an Rikagu D-max 2200 PC model diffractometer (Dokuz Eylül University) working at 40 kV and 30 mA with CuK_α radiation at a wavelength of 1.54 \AA . The patterns were collected with a scanning velocity of $2^\circ/\text{min}$ between $3 - 90^\circ$ 2θ angle intervals. The ICDD PDF-2 database was used for phase identification.

RESULTS AND DISCUSSION

The particle size distribution of the raw materials should be under $63 \mu\text{m}$ for industrial applications [33]. A total of 95.21% of the OG, 82.01% of the FA, 89.57% of the TW, and 98.52% of the RC fall below this limit. ZrO_2 and ZnO are the opacifiers of OG. The fundamental oxides of FA and RC are SiO_2 , Al_2O_3 , and Fe_2O_3 . The high contents of K_2O (3.31%) and CaO (3.21%) in RC indicate the presence of illite and carbonates. The flow time and densities of all batches range from 20–30 sec and $1.6 - 1.7 \text{ g/cm}^3$, respectively, which are consistent with the values of dipping glazes [34].

The pH values of the batches were between 10 and 10.5. The pH value of well-dispersed suspensions lies between 10 and 11 because of the deprotonation of the surface hydroxyl groups of silica and alumina, which causes a negative surface charge [35]. Ceramic tiles are heated between 1000 and

1200°C in the industry due to the number of alkali oxides and the particle size distribution of the raw materials in glazes. The heating temperature of 1150°C was adequate for the vitrification of fluxing oxides of raw materials in this study.

Table 7 shows WA percentages and SH ranges (Mohs' scale) of the heated bodies. According to ASTM C 618 [36], the FA used in this study is class F, since the sum of the percentages of SiO₂, Al₂O₃ and Fe₂O₃ are above 70% and the CaO content is lower than 10%. Also, it contains 12.36% ferric oxide. The addition of FA may influence the gradual decline of WA values from 0.52% to 0.27%. Fe₂O₃ is an effective fluxing oxide on for densification behavior of ceramic tiles as an alkali metal oxide [37]. The fluidity of the vitreous phase at sintering temperatures may increase with the reaction of ferric ions with glaze components, frits, or ceramic tiles [38]. The open micropores of the tiles may be filled with the vitreous phase which will decrease WA values as a result.

Similarly, RC subsumes large quantities of fluxing oxides but a higher LOI value (9.42%) implying the occurrence of clay minerals, hydroxides, and organic matter in its structure [39, 40]. The Pfefferkorn plasticity and Hausner ratio of RC are 24.4 and 1.32 respectively. The WA values of the RC group were less than those of OG. Both the fluxing oxide content and low plasticity of RC may increase the amount of liquid phase during sintering and decrease the porosity and WA [41]. WA values were also reduced when FA and RC are both used in the FC groups.

SH is a way of guessing the durability of a glazed surface. The Mohs values of all groups are in the range of 6 and 7. In general, the SH of a ceramic surface is desired to be greater than 6.5 for industrial and commercial applications [42]. On the other hand, the possibility of recognizing the scratches caused by the standard may not be precise, especially on light colored and matte glazes; therefore, the Vickers method will be more appropriate for determining wear resistance.

The waste materials did not cause any incompatibility in means of thermal expansion between biscuit and glaze. No cracks or crazing were seen on the surface of the samples between 100 and 180°C. According to Arcasoy [43] and Yalçın and Nevin [44] glazed ceramics that are resistant to thermal shock at 180°C are usable for two or three years without crazing.

Glazed surfaces are exposed to abrasive materials because of regular cleaning and environmental conditions. Most glazed tiles are resistant to acidic and alkaline solutions except hydrofluoric acid and salts containing fluoride ions. If a glazed surface is affected by an acidic solution, there will

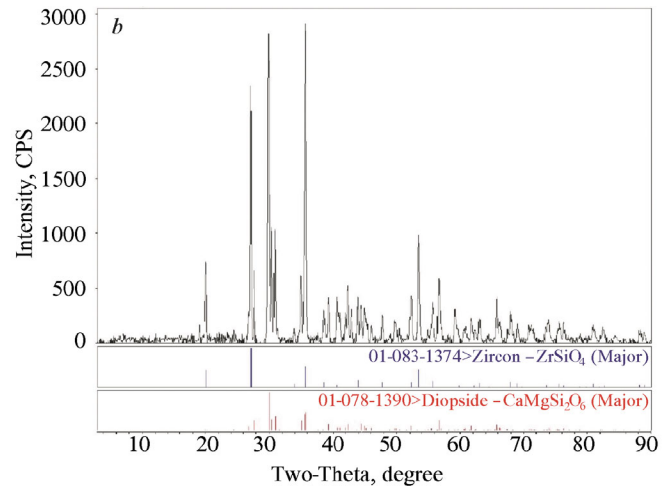


Fig. 3. SEM microstructure (a) and XRD pattern (b) of OG.

be an exchange reaction between the proton of an acid and the metal in the glaze network [45]; if it is affected by an alkaline solution the glaze network will decompose because of the breaking of the Si–O bonds [46]. None of the batches are affected by chemical solutions as no color change or dullness is seen on the surfaces. The lines drawn on the surfaces are erased easily by wet cloth, implying the A-class due to TS EN ISO 10545-13 [29].

Staining is related to the porosity and roughness of a surface where dirt will accumulate in time, displaying poor mechanical properties [47, 48]. Inhomogeneous dipping facilitates soiling. Glazed tiles are resistant to staining because of the smooth coating which decreases porosity [49, 50] (Table 7). The tiles are consistent with the fifth class of TS EN ISO 10545-14 [30] as the dirt is cleaned off easily by hot water.

The incomplete melting of oxides (devitrification) and trapped air bubbles formed during this process cause crystallization when cooling. These insoluble particles lead to more

TABLE 7. WA Percentage and SH of the Batches

Batch name	OG	FA0.5	FA1	FA2	FA3	FA4	RC0.5	RC1	RC2	RC3	RC4	F4C0.5	F0.5C4	F2C2
WA, %	0.52	0.48	0.37	0.33	0.29	0.27	0.32	0.26	0.22	0.20	0.18	0.34	0.32	0.27
SH, Mohs	6–7	6	6	6	6	6	6–7	6–7	6–7	6–7	6–7	6	6–7	6

scattering and reflection of the incident light and therefore opacity [51]. Additionally, the ratio of SiO_2 to Al_2O_3 plays an important role in opaqueness which should be between 8 : 1 and 10 : 1, especially in zirconia containing glazes [52]. The ratio is between 8.71 and 8.85 for all batch types which is in good agreement with the high L^* values (Table 8). The utilization wastes had no effect on the whiteness of the glaze. All a^* values are negative and b^* values are positive. Tiles display a light green–yellow color. The a^* values of the FA and RC groups are higher than those of OG which may originate from the redness of ferric oxide as the FA groups indicate more positive values with higher Fe_2O_3 contents.

OG, FA4, RC4 and F2C2 samples were selected to elucidate the microstructure and crystalline phases of each group via SEM and XRD analysis respectively (Fig. 3 – 6). Zircon was the major phase for all groups. The peak density of RC4 is stronger than the others, indicating a dense zircon layer (Fig. 5). The zircon crystals, as slender prisms, could be formed by partial dissolution of ZrO_2 in silicate melt causing both high opacity and dullness. The opacity values are greater than 90 and gloss values are in the range of 27 – 45%. Additionally, low contents of B_2O_3 and ZnO may help the growth of zircon crystals.

On the other hand, crystallization of zircon can be impeded by the presence of Fe_2O_3 [53] and if the molar ratio of MgO to CaO is more than 0.2 [54]. They both gave rise to the formation of another phase, diopside containing small, rounded crystals, as can be seen in the OG, FA4 and F2C2 samples. In some cases, augite phase might occur when Fe^{+3} ions caused the breaking of Si–O–Si bonds of the glaze network as reported by Erol, et al. [55], which was identified only on F2C2.

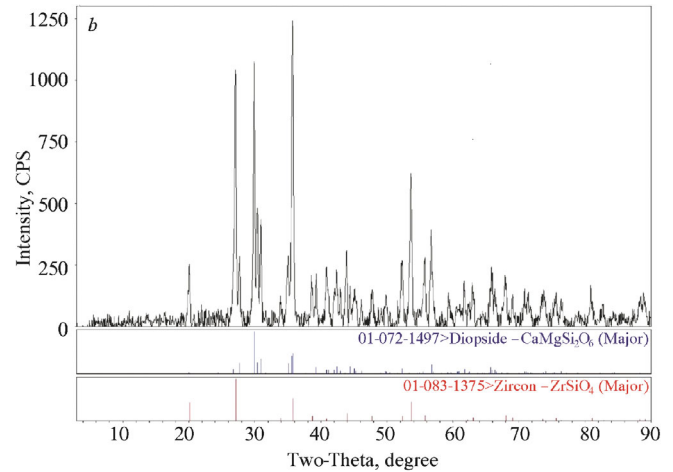


Fig. 4. SEM microstructure (a) and XRD pattern (b) of FA4.

CONCLUSIONS

Experimental glazes were prepared by blending OG with waste materials and FA and RC in different proportions. TW was used to decrease the sintering temperature. Biscuit tiles were dipped in the glaze mixtures and heated at 1150°C and subjected to mechanical and microstructural tests.

TABLE 8. Color Variation of the Batches

Batch name	L^*	a^*	b^*	ΔL^*	Δa^*	Δb^*	ΔL^2	Δa^2	Δb^2	ΔE^2	ΔE
OG	93.03	-1.45	2.44								
FA0.5	92.48	-1.36	3.12	0.55	-0.09	-0.68	0.30	0.01	0.46	0.77	0.88
FA 0.7	92.51	-1.23	3.18	0.52	-0.22	-0.74	0.27	0.05	0.55	0.87	0.93
FA1	92.49	-1.21	3.22	0.54	-0.24	-0.78	0.29	0.06	0.61	0.96	0.98
FA2	92.62	-1.18	3.28	0.41	-0.27	-0.84	0.17	0.07	0.71	0.95	0.97
FA3	92.95	-1.19	3.33	0.08	-0.26	-0.89	0.01	0.07	0.79	0.87	0.93
FA4	92.74	-1.22	3.34	0.29	-0.23	-0.90	0.08	0.05	0.81	0.95	0.97
RC0.5	93.47	-1.25	2.85	-0.44	-0.20	-0.41	0.19	0.04	0.17	0.4	0.63
RC0.7	93.62	-1.27	2.93	-0.59	-0.18	-0.49	0.35	0.03	0.24	0.62	0.79
RC1	92.97	-1.38	3.18	0.06	-0.07	-0.74	0	0	0.55	0.56	0.75
RC2	92.73	-1.40	3.34	0.30	-0.01	-0.90	0.09	0	0.81	0.90	0.95
RC3	92.81	-1.42	3.37	0.22	0.07	-0.93	0.05	0	0.86	0.92	0.96
RC4	92.88	-1.44	3.31	0.15	0.15	-0.87	0.02	0.02	0.76	0.80	0.90
F4C0.5	93.29	-1.44	3.18	-0.26	-0.01	-0.74	0.07	0	0.55	0.62	0.78
F0.5C4	92.75	-1.27	3.13	0.28	-0.18	-0.69	0.08	0.03	0.48	0.59	0.77
F2C2	92.64	-1.22	3.19	0.39	-0.23	-0.75	0.15	0.05	0.56	0.77	0.88

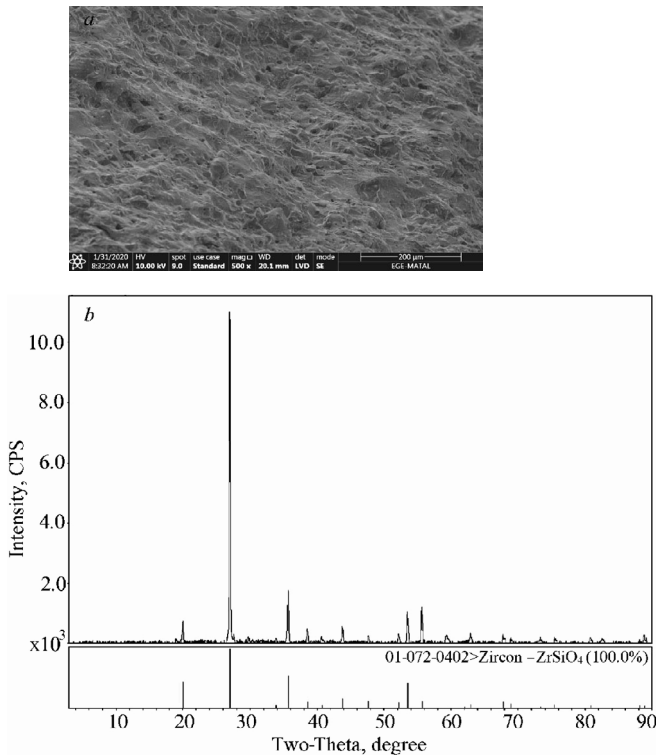


Fig. 5. SEM microstructure (a) and XRD pattern (b) of RC4.

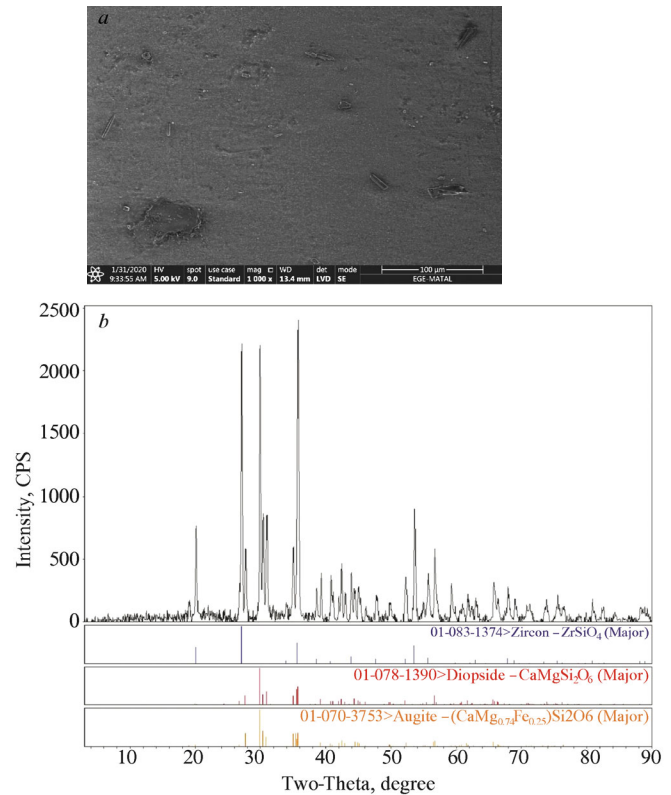


Fig. 6. SEM microstructure (a) and XRD pattern (b) of F2C2.

These specific conclusions can be listed as follows:

- The fluxing oxides and the ferric oxide in FA and RC gave rise to a decrease in the WA value of OG in all batches.
- The SH of all groups is in the range of 6 and 7, but more accurate results can be obtained with another method since one can be mistaken with the naked eye.
- All groups passed the Harcourt test between 100 and 180°C degrees. The glaze and the biscuit tiles were still congruent after the addition of FA, RC, and TW. No cracks or crazing were seen on the surface of the tiles and the tiles were resistant to chemicals and staining agents compatible with class A of TSE EN ISO 10545-13 and TSE EN ISO 10545-14.
- The whiteness values were between 92 and 93 showing high opacity. All a^* values were negative whereas b^* values were positive. The light greenish-yellow and red colors might originate due to the ferric ions of FA and RC.
- Due to the SEM and XRD results, the main phase of all groups was zircon. The diopside phase was identified on OG, FA4 and F2C2 surfaces while augite was determined only on the F2C2 sample.
- All waste materials can be used in producing opaque glazes.

REFERENCES

1. M. Çakı, S. Y. Kaya and B. Günhan, "The use of glass waste in stoneware glazes," *Ceram. Tech.*, **37**, 14 – 19 (2013).
2. <http://www.globalwastemanagementconference.com>
3. K. Dana, J. Dey and S. K. Das, "Synergistic effect of fly ash and blast furnace slag on the mechanical strength of traditional porcelain tiles," *Ceram. Int.*, **31**, 147 – 152 (2005).
4. R. R. Menezes, L. N. L. Santana, G. A. Neves and H. C. Ferreira, *Environmental Contamination*, e-book (2012).
5. Y. Demirel and Y. Çağlar, "Recovery of phosphogypsum in economy in building material waste," *J. Fac. Eng. Archt. Gazi Univ.*, **30**(4), 743 – 750 (2015) (in Turkish).
6. B. Karasu, G. Kaya, R. Kozulu, *Proc. the 1st Int. Boron Symp.*, Kütaahya, Turkey (2002), p. 193 (in Turkish).
7. R. K. D. Obe, J. de Brito, G. S. Ghataora and C. Q. Lye, *Sustainable Construction Materials*, Woodhead Publishing, Cambridge (2018).
8. <https://www3.epa.gov/ttnchie1/ap42/ch11/final/c11s07.pdf>
9. T. Pradell and J. Molera, "Ceramic technology. How to characterize ceramic glazes," *Archaeol. Anthropol. Sci.*, **12**(189), 1 – 28 (2020).
10. S. R. Bragança and C. P. Bergmann, *4th Mercosur Cong. Process Syst. Eng. and 2nd Mercosur Cong. Chem. Eng. Proc. ENPROMER*, Rio de Janeiro, Brazil (2005).
11. M. S. Sultana, A. N. Ahmed, M. N. Zaman, M. A. Rahman, P. K. Biswas and P. K. Nandy, "Utilization of hard rock dust with red clay to produce roof tiles," *J. Asian Ceram. Soc.*, **3**, 22 – 26 (2015).
12. *TS 639/T1, Fly Ash in Concrete* (1998), pp. 1 – 14.
13. S. Yadav, V. C. Pandey and L. Singh, "Ecological restoration of fly ash-dumped area: Challenges and Opportunities," *Land Degrad. Dev.* (2021) (in press). <https://doi.org/10.22541/au.161778478.83466968/v1>

14. O. Özdemir and M. S. Çelik, "Characterization and recovery of lignitic fly ash byproducts from the Tuncbilek power station," *Can. Metall. Q.*, **41**(2), 143 – 150 (2002).
15. https://www.epj.conferences.org/articles/epjconf/pdf/2019/01/epjconf_autfg18_00014.pdf.
16. K. L. Lin, "Feasibility study of using brick made from municipal solid waste incinerator fly ash slag," *J. Hazard. Mater.*, **137**(3), 1810 – 1816 (2006).
17. A. Zimmer and C. P. Bergman, "Fly ash of mineral coal as raw material," *J. Waste Manag.*, **27**(1), 59 – 68, (2007).
18. M. Erol, S. Küçükbayrak and A. Ersoy Meriçboyu, "Comparison of the properties glass, glass-ceramic and ceramic materials produced from coal fly ash," *J. Hazard. Mater.*, **153**(1–2), 418 – 425 (2008).
19. D. Rhodes, *Clay and Glazes for the Potter*, Chilton Book Company, West Chester (1973).
20. S. J. Yoo, S. I. Lee, D. H. Kwak, K. G. Kim, K. J. Hwang and J. W. Lee, "Photocatalytic degradation of methylene blue and acetaldehyde by TiO₂/glaze coated porous red clay tile," *Korean J. Chem. Eng.*, **25**(5), 1232 – 1238 (2008).
21. S. J. G. Sousa and J. N. F. Holanda, "Characterization of non-calcareous thin red clay from south-eastern Brazil: applicability in wall tile manufacture," *Ceramica*, **58**(345), 29 – 35 (2012).
22. T. Kavas, "Use of boron waste as a fluxing agent in production of red mud brick," *Build. Environ.*, **41**(12), 1779 – 1783 (2006).
23. K. Pfefferkorn, "Ein Beitrag zur Bestimmung der Plastizität in Tonen und Kaolinen," *Sprechsaaal*, **57**, 297 – 299 (1924).
24. F. A. Andrade, H. A. Al-Qureshi and D. Hotza, "Measuring the plasticity of clays: A review," *Appl. Clay Sci.*, **51**(1–2), 1 – 7 (2011).
25. https://acikders.ankara.edu.tr/pluginfile.php/69409/mod_resource/content/0/4.Hafta_Toz%20Teknolojisi%20Mikromeritik%20ve%20Reçeteleri.pdf (in Turkish).
26. *ISO 10545-3 Ceramic Tiles – Part 3, Determination of Water Absorption Apparent Porosity, Apparent Relative Density, and Bulk Density* (2018), pp. 1 – 6.
27. *ISO 13630-13 Ceramic Tiles – Part 13, Determination of Scratch Hardness of Surfaces According to Mohs* (2006), pp. 1 – 4.
28. *ISO 10545-9 Ceramic Tiles – Part 9, Determination of Resistance to Thermal Shock* (2013), pp. 1 – 6.
29. *ISO 10545-13 Ceramic Tiles – Part 13, Determination of Chemical Resistance* (2016), pp. 1 – 9.
30. *ISO 10545-14 Ceramic Tiles – Part 14, Determination of Resistance to Stains* (2015), pp. 1 – 16.
31. *ISO 10545-16 Ceramic Tiles – Part 16, Determination of Small Color Differences* (2010), pp. 1 – 12.
32. <https://www.hunterlab.com/en/>
33. <https://digitalfire.com/material/list>
34. <https://www.spectrumglazes.com>
35. N. U. Koçkal, "Properties and microstructure of porous ceramic bodies containing fly ash," *J. Build. Phys.*, **35**(4), 338 – 352 (2011).
36. *ASTM C 618, Standard Specification for Coal Fly Ash and Raw or Calcined Natural Pozzolan for Use in Concrete* (2019), pp. 1 – 5.
37. B. Rajamannan, C. K. Sundaram, G. Viruthagiri and N. Shanmugam, "Effects of fly ash addition on the mechanical and other properties of ceramic tiles," *IJLRST*, **2**(1), 486 – 491 (2013).
38. E. Özel and S. Turan, "Production and characterization of iron-chromium pigments and their interactions with transparent glazes," *J. Eur. Ceram. Soc.*, **23**(12), 2097 – 2104 (2003).
39. L. Moussa, E. Srasra and K. Bouzouita, "Stabilisation of clay suspension used in Tunisian ceramics," *Miner. Petrography Acta*, **35-A**, 147 – 159 (1992).
40. H. Baccour, M. Medhioub, F. Jamoussi and T. Mhiri, "Densification behavior of a red firing Tunisian Triassic clay," *Am. J. Appl. Sci.*, **5**(3), 263 – 269, (2008).
41. C. M. F. Vieira and S. N. Monteiro, "Incorporation of solid wastes in red ceramics: an updated review," *Rev. Mater.*, **14**(3), 881 – 905, (2009).
42. M. W. Wine, *Patent 5,693,395* (1997).
43. A. Arcasoy, *Ceramic Technology*, Gençlik Bookstore, Istanbul (1983) (in Turkish).
44. N. Yalçın and V. Sevinç, "Utilization of bauxite waste in ceramic glazes," *Ceram. Int.*, **26**(5), 485 – 493 (2000).
45. W. D. Kingery, Bowen H. K. and D. R. Uhlmann, *Introduction to Ceramics*, John Wiley & Sons, Nashville (1976).
46. T. Kopar and V. Ducman, "Low-vacuum SEM analyses of ceramic tiles with emphasis on glaze defects characterization," *Mater. Charact.*, **58**(11 – 12), 1133 – 1137 (2007).
47. L. Sánchez-Muñoz, S. da S. Cava, C. A. Paskocimas, E. Cerisuelo, E. Longo and J. B. Carda, "Influence of raw materials composition on the vitrification process of ceramic tiles," *Ceramica*, **48**(307), 137 – 145 (2002).
48. A. C. S. Alcântara, M. S. S. Beltrão, H. A. Oliveira, I. F. Gimenez and L. S. Barreto, "Characterization of ceramic tiles prepared from two clays from Sergipe Brazil," *Appl. Clay Sci.*, **39**(3 – 4), 160 – 165 (2008).
49. P. M. Tenorio Cavalcante, M. Dondi, G. Ercolani, G. Guarini, C. Melandri, M. Raimondo and E. R. Almendra, "The influence of microstructure on the performance of white porcelain stoneware," *Ceram. Int.*, **30**(6), 953 – 963 (2004).
50. M. Dondi, G. Ercolani, G. Guarini, C. Melandri, M. Raimondo, E. R. Almendra, and P. M. Tenorio Cavalcante, "The role of surface microstructure on the resistance to stains of porcelain stoneware tiles," *J. Eur. Ceram. Soc.*, **25**(4), 357 – 365 (2005).
51. E. Sánchez, M. J. Ibáñez, J. García-Ten, M. F. Quereda, I. M. Hutchings and Y. M. Xu, "Porcelain tile microstructure: Implications for polished tile properties," *J. Eur. Ceram. Soc.*, **26**(13), 2533 – 2540 (2006).
52. S. Stefan and B. Svetlan, *Keramik-Glasuren: Chemie. Technologie und Anwendung*, Bauverlag, West Germany (1988).
53. M. Romero, J. M. Rincon, and A. Acosta, "Crystallization of zirconium-based glaze for tile coating," *J. Eur. Ceram. Soc.*, **23**(10), 1629 – 1635 (2003).
54. L. Fröberg, T. Kronberg, L. Hupa and M. Hupa, "Influence of firing parameters on phase composition of raw glazes," *J. Eur. Ceram. Soc.*, **27**(2 – 3), 1671 – 1675 (2007).
55. M. Erol, S. Küçükbayrak and A. Ersoy Meriçboyu, "Production of glass-ceramics obtained from industrial wastes by means of controlled nucleation and crystallization," *Chem. Eng. J.*, **132**, 335 – 343 (2007).